RSC Advances

PAPER

View Article Online
View Journal | View Issue

Cite this: *RSC Adv.*, 2017, **7**, 17650

A single colorimetric sensor for multiple targets: the sequential detection of Co^{2+} and cyanide and the selective detection of Cu^{2+} in aqueous solution†

Hyo Jung Jang, Tae Geun Jo and Cheal Kim*

Received 8th February 2017
Accepted 16th March 2017

DOI: 10.1039/c7ra01580a

rsc.li/rsc-advances

A new highly selective and multifunctional chemosensor **1** for the detection of Co^{2+}, Cu^{2+} and CN^-, based on 4-diethylaminosalicyl aldehyde and thiophene-2-carbohydrazide moieties, was designed and synthesized. **1** could simultaneously detect both Co^{2+} and Cu^{2+} by changing its color from colorless to yellow in aqueous solution. The binding modes of **1** to Co^{2+} and Cu^{2+} were determined to be a 2 : 1 complexation stoichiometry through job plot and ESI-mass spectrometry analysis. The detection limits (0.19 μM and 0.13 μM) of **1** for Co^{2+} and Cu^{2+} were lower than the DEP guideline (1.7 μM) of Co^{2+} and the WHO guideline (31.5 μM) of Cu^{2+} for drinking water. Importantly, **1** could detect and quantify Co^{2+} and Cu^{2+} in real water samples. Moreover, the resulting Co^{2+}-2·**1** complex sensed cyanide through naked-eye, showing recovery from Co^{2+}-2·**1** to **1**. The sensing mechanisms of Cu^{2+} by **1** were explained by theoretical calculations.

1. Introduction

The development of colorimetric chemosensors for detecting metal ions has received considerable interest in chemical, environmental and biological areas.[1–6] Cobalt is an important trace element found in rocks, minerals, soils and seawater, and plays a critical role in biological systems.[7–11] It is well known that Co^{2+} is an important component of vitamin B12 and other biological compounds, and also plays a critical role in the metabolism of iron and the synthesis of hemoglobin.[12–14] However, exposure to high levels of cobalt can lead to toxicological effects, including heart disease, thyroid enlargement, asthma, decreased cardiac output, lung disease, dermatitis and vasodilation.[15–22] For these reasons, a highly selective and sensitive determination of trace amounts of Co^{2+} is necessary in biological and environmental systems.

Copper is the third most abundant metal in the human body.[23–26] It functions as a significant cofactor in the process of superoxide dismutase, cytochrome *c* oxidase and tyrosinase.[27,28] However, excess intake of Cu^{2+} can trigger adverse health effects such as Alzheimer's, Menke's, Parkinson's and Wilson's diseases.[29–31] The World Health Organization (WHO) has recommended the maximum limit of copper in drinking water at 2 ppm (31.5 μM).[32,33] Therefore, much effort has been devoted to the development of various chemosensors for Cu^{2+} detection.[34–40]

Cyanide has received attention, because it is known as one of the most rapidly acting and strong poisons. The toxicity is caused by its propensity to bind to the iron in cytochrome *c* oxidase, interfering with electron transport and resulting in hypoxia.[41–44] In spite of the toxicity, cyanide has been required in diverse industrial processes such as raw materials for synthetic fibers, resins, herbicides, and the gold-extraction process.[45–48] For these reasons, the development of chemosensors for the recognition and detection of cyanide has also received considerable attention.

Many analytical methods for the detection of Co^{2+}, Cu^{2+}, and CN^- have been developed such as atomic absorption-emission spectrometry, inductively coupled plasma atomic emission spectroscopy and electrochemical methods. However, the methods demand expensive equipment, highly trained operators and complicated pre-treatment for routine monitoring and application.[49] On the contrary to these analytic methods, colorimetric methods have the several merits such as low cost, high sensitivity, and easy monitoring of the target ions.[50]

Herein, we report on the synthesis and sensing properties of a new thiophene-2-carbohydrazide based chemosensor **1**. The chemosensor **1** could simultaneously detect both Co^{2+} and Cu^{2+} ions *via* color changes from colorless to yellow in aqueous solution. In addition, the *in situ* formed Co^{2+}-2·**1** complex exhibited highly selective recognition of CN^- through a color change from yellow to colorless in aqueous solution. The

Department of Fine Chemistry and Department of Interdisciplinary Bio IT Materials, Seoul National University of Science and Technology, Seoul 139-743, Korea. E-mail: chealkim@seoultech.ac.kr; Fax: +82-2-973-9149; Tel: +82-2-970-6693

† Electronic supplementary information (ESI) available: Supplementary data (experimental procedures and additional experimental data) associated with this article can be found. See DOI: 10.1039/c7ra01580a

sensing mechanisms of **1** toward Co^{2+}, Cu^{2+}, and CN^- were explained by using various analytical methods.

2. Experimental

2.1. Materials and equipment

All the solvents and reagents (analytical and spectroscopic grade) were purchased from Sigma-Aldrich. Absorption spectra were recorded at room temperature using a Perkin Elmer model Lambda 25 UV/vis spectrometer. ^1H and ^{13}C NMR spectra were recorded on a Varian 400 MHz and 100 MHz spectrometer and chemical shifts (δ) were recorded in ppm. Electro spray ionization mass spectra (ESI-MS) were collected on a Thermo Finnigan (San Jose, CA, USA) LCQ™ Advantage MAX quadrupole ion trap instrument by infusing samples directly into the source using a manual method. Spray voltage was set at 4.2 kV, and the capillary temperature was at 80 °C. Elemental analysis for carbon, nitrogen, and hydrogen was carried out using a Flash EA 1112 elemental analyzer (thermo) at the Organic Chemistry Research Center of Sogang University, Korea.

2.2. Synthesis of sensor 1

A solution of thiophene-2-carbohydrazide (0.145 g, 1 mmol) was added to quinolone-2-carboxaldehyde (0.19 g, 1.2 mmol) in ethanol (5 mL). The reaction solution was stirred for 12 h at room temperature. A white precipitate formed was filtered, washed several times with methanol and diethyl ether, and dried in vacuum to afford the pure white solid. Yield 0.24 g (85%); ^1H NMR (400 MHz DMSO-d_6, ppm): δ 12.17 (s, 1H), 8.59 (s, 1H), 8.44 (d, J = 8 Hz, 1H), 8.31 (s, 1H), 8.20 (s, 1H), 8.09 (s, 1H), 8.02 (m, J = 24 Hz, 3H), 7.79 (t, J = 16 Hz, 1H), 7.63 (t, J = 12 Hz, 1H), 7.25 (t, J = 8 Hz, 1H); ^{13}C NMR (100 MHz, DMSO-d_6, 25 °C): δ = 152.56, 149.86, 142.08, 140.39, 137.69, 135.36, 134.74, 134.11, 133.22, 132.59, 122.72. ESI-MS: m/z [**1** + H^+]$^+$ calcd 282.07, found, 282.00.

2.3. UV-vis titration measurements of Co^{2+} and Cu^{2+}

Sensor **1** (0.16 mg, 0.001 mmol) was dissolved in dimethyl sulfoxide (DMSO, 1 mL) and 60 μL of this solution (1 mM) was diluted with 2.94 mL of bis–tris buffer/DMSO (95/5, 10 mM bis–tris, pH = 7.0) to make the final concentration of 20 μM. $Co(NO_3)_2 \cdot 6H_2O$ (1.45 mg, 0.005 mmol) was dissolved in bis–tris buffer (1 mL) and 0.6–2.25 μL of this Co^{2+} solutions (5 mM) were transferred to the sensor **1** solution (20 μM) prepared above. After mixing them for a few seconds, UV-vis spectra were taken at room temperature. The same experimental procedures were also carried out for Cu^{2+} ion.

2.4. Job plot measurements of Co^{2+} and Cu^{2+}

Sensor **1** (0.16 mg, 0.001 mmol) was dissolved in DMSO (1 mL) and 600 μL of the sensor **1** (1 mM) was diluted to 39.4 mL bis–tris buffer/DMSO (95/5, v/v) solution to make to final concentration of 20 μM. 2.7, 2.4, 2.1, 1.8, 1.2, 0.9, 0.6 and 0.3 mL of the sensor **1** solution were taken and transferred to quartz cells. 40 μL of the Co^{2+} solution (20 mM) was diluted to 39.6 mL buffer/DMSO (95/5, v/v) solution. 0.3, 0.6, 0.9, 1.2, 1.5, 1.8, 2.1, 2.4 and 2.7 mL of the Co^{2+} solution were transferred to each sensor **1** solution. Each cell had a total volume of 3 mL. After mixing them for a few seconds, UV-vis spectra were taken at room temperature. The same experimental procedures were also carried out for Cu^{2+} ion.

2.5. Competition experiments of Co^{2+} and Cu^{2+}

Sensor **1** (0.16 mg, 0.001 mmol) was dissolved in DMSO (1 mL) and 60 μL of this solution (1 mM) was diluted with 2.94 mL of bis–tris buffer/DMSO (95/5, v/v) to make the final concentration of 20 μM. MNO_3 (M = Na, K, Ag, 0.02 mmol) or $M(NO_3)_2$ (M = Mn, Fe, Co, Ni, Cu, Zn, Cd, Hg, Mg, Ca, Pb, 0.02 mmol) or $M(NO_3)_3$ (M = Fe, Cr, Al, Ga, In, 0.02 mmol) were separately dissolved in bis–tris buffer (1 mL). 2.25 μL of each metal-ion solution (20 mM) was taken and added to 3 mL of the solution of sensor **1** (20 μM) to give 7.5 equiv. Then, 2.25 μL of Co^{2+} solution (20 mM) was added into the mixed solution of each metal ion and **1** to make 7.5 equiv. After mixing them for a few seconds, UV-vis spectra were taken at room temperature. The same experimental procedures were also carried out for Cu^{2+} ion.

2.6. pH effect tests of Co^{2+} and Cu^{2+}

A series of solutions with pH values ranging from 2 to 12 were prepared by mixing sodium hydroxide solution and hydrochloric acid. After the solution with a desired pH was achieved, sensor **1** (0.16 mg, 0.001 mmol) was dissolved in DMSO (1 mL), and then 60 μL of the sensor (1 mM) was diluted with 2.94 mL of bis–tris buffer/DMSO (95/5, v/v) to make the final concentration of 20 μM. $Co(NO_3)_2 \cdot 6H_2O$ (5.82 mg, 0.02 mmol) was dissolved in bis–tris buffer (1 mL). 2.25 μL of the Co^{2+} solution (20 mM) was transferred to each sensor solution (20 μM) prepared above. After mixing them for a few seconds, UV-vis spectra were taken at room temperature. The same experimental procedures were also carried out for Cu^{2+} ion.

2.7. Determination of Co^{2+} and Cu^{2+} in water samples

UV-vis spectral measurements of water samples containing Cu^{2+} were carried by adding 60 μL solution of the sensor **1** (1 mM) and 0.3 mL of 100 mM bis–tris buffer stock solution to 2.64 mL sample solutions. After mixing them for a few seconds, UV-vis spectra were taken at room temperature. The same experimental procedures were also carried out for Cu^{2+} ion.

2.8. Theoretical calculations

All theoretical calculations were performed by using Gaussian 03 program.[51] The molecular geometries were optimized by the Density Functional Theory (DFT) calculations based on the hybrid exchange-correlation functional B3LYP.[52,53] The 6-31G** basis set[54,55] was used for the main group (C, H, O and N) and the Lanl2DZ effective core potential (ECP)[56,57] was considered for Cu^{2+}. The vibrational frequency calculations were carried out. There was no imaginary frequency for the optimized geometries of **1** and Cu^{2+}-2·**1**, indicating that these structures were local energy minima. For all calculations, the solvent effect

of water was considered by using the Cossi and Barone's CPCM (conductor-like polarizable continuum model).[58,59] The twenty lowest singlet states were calculated by using Time-Dependent Density Functional Theory (TD/DFT). The GaussSum 2.1 (ref. 60) was used to calculate the contributions of molecular orbitals in electronic transition.

2.9. UV-vis titration measurements of Co^{2+}-2·1 with CN^-

Sensor **1** (0.16 mg, 0.001 mmol) was dissolved in DMSO (1 mL) and 60 μL of this solution (1 mM) was diluted with 2.94 mL of bis–tris buffer/DMSO (95/5, 10 mM bis–tris, pH = 7.0) to make the final concentration of 20 μM. 2.25 μL of Co^{2+} solution (20 mM) was transferred to each sensor solution (20 μM) to give 0.75 equiv. Then, tetraethylammonium cyanide (16.56 mg, 0.1 mmol) was dissolved in bis–tris (100 mM, 1 mL) and 1.8–19.8 μL of this CN^- solutions (100 mM) were transferred to Co^{2+}-2·**1** solution (20 μM) to give 33 equiv. After mixing them for a few seconds, UV-vis spectra were taken at room temperature.

2.10. Job plot measurements of Co^{2+}-2·1 with CN^-

Sensor **1** (0.16 mg, 0.001 mmol) was dissolved in DSMO (1 mL) and 600 μL of the sensor **1** (1 mM) were diluted to 39.4 mL bis–tris buffer/DMSO (95/5, v/v) solution to make the final concentration of 20 μM. $Co(NO_3)_2 \cdot 6H_2O$ (5.94 mg, 0.02 mmol) was dissolved in bis–tris buffer (5 mL) and 40 μL of this Co^{2+} solution (20 mM) was transferred to the sensor solution (20 μM) to make Co^{2+}-2·**1** complex. 2.7, 2.4, 2.1, 1.8, 1.2, 0.9, 0.6 and 0.3 mL of the Co^{2+}-2·**1** solution were taken and transferred to quartz cells. Tetraethylammonium cyanide (16.56 mg, 0.1 mmol) was dissolved in bis–tris (100 mM, 1 mL). 8 μL of the cyanide solution (100 mM) was diluted to 39.992 mL bis–tris buffer solution. 0.3, 0.6, 0.9, 1.2, 1.5, 1.8, 2.1, 2.4 and 2.7 mL of the diluted cyanide solution were transferred to each Co^{2+}-2·**1** solution. Each cell had a total volume of 3 mL. After mixing them for a few seconds, UV-vis spectra were taken at room temperature.

2.11. Competition of Co^{2+}-2·1 toward various anions

Sensor **1** (0.16 mg, 0.001 mmol) was dissolved in DMSO (1 mL) and 60 μL of this solution (1 mM) was diluted with 2.94 mL of bis–tris buffer/DMSO (95/5, v/v) to make the final concentration of 20 μM. $Co(NO_3)_2 \cdot 6H_2O$ (5.94 mg, 0.02 mmol) was dissolved in bis–tris buffer (1 mL). 2.25 μL of this Co^{2+} solution (20 mM) was transferred to the **1** solution (20 μM) to make Co^{2+}-2·**1** complex. Then, tetraethylammonium salts of F^-, Cl^-, Br^- and I^-, and tetrabutylammonium salts of OAc^-, $H_2PO_4^-$, N_3^-, SCN^- and BzO^- (0.1 mmol), and sodium salts of S^{2-} (0.1 mmol) were separately dissolved in bis–tris buffer (1 mL). 18 μL of each anion solution (100 mM) was taken and added into each Co^{2+}-2·**1** complex solution prepared above to make 30 equiv. Then, 18 μL of the tetraethylammonium cyanide solution (100 mM) was added into the mixed solution of each anion and Co^{2+}-2·**1** complex to make 30 equiv. After mixing them for a few seconds, UV-vis spectra were taken at room temperature.

2.12. pH effect test of Co^{2+}-2·1 with CN^-

A series of solutions with pH values ranging from 2 to 12 were prepared by mixing sodium hydroxide solution and hydrochloric acid. After the solution with a desired pH was achieved, 60 μL of the **1** solution (1 mM) and 2.25 μL of the $Co(NO_3)_2$ solution (20 mM) were dissolved in bis–tris buffer/DMSO (95/5, v/v, pH 2–12), respectively. Then, 18 μL of tetraethylammonium cyanide solution (100 mM) was transferred to Co^{2+}-2·**1** complex solution prepared above. After mixing them for a few seconds, UV-vis spectra were taken at room temperature.

3. Results and discussion

Sensor **1** was obtained by the combination of thiophene-2-carbohydrazide and quinolone-2-carboxaldehyde with 85% yield in ethanol (Scheme 1), and characterized by ^1H NMR and ^{13}C NMR, ESI-mass spectrometry, and elemental analysis.

3.1. Absorption spectroscopic studies of 1 toward Co^{2+} and Cu^{2+}

The colorimetric selectivity of sensor **1** toward various metal ions was conducted in bis–tris buffer/DMSO (95/5, v/v, pH = 7) (Fig. 1a). When 0.75 equiv. of various metal ions such as Al^{3+}, Ga^{3+}, In^{3+}, Zn^{2+}, Cd^{2+}, Cu^{2+}, Fe^{2+}, Fe^{3+}, Mg^{2+}, Cr^{3+}, Hg^{2+}, Ag^+, Co^{2+}, Ni^{2+}, Na^+, K^+, Ca^{2+}, Mn^{2+} and Pb^{2+} were added to **1**, only both Co^{2+} and Cu^{2+} showed distinct spectral changes at 400 nm and instant color changes from colorless to yellow, while other metal ions did not show any change in absorbance spectrum and color (Fig. 1b). These results suggested that the sensor **1** could be used as a "naked-eye" chemosensor for Co^{2+} and Cu^{2+} in aqueous media.

First of all, we conducted the UV-vis titration to examine the concentration-dependent signaling of **1** toward Co^{2+} (Fig. 2). On the gradual addition of Co^{2+} to a solution of **1**, the absorption band at 325 nm significantly decreased, and a new band at 400 nm gradually reached a maximum at 0.75 equiv. of Co^{2+}. A clear isosbestic point was observed at 356 nm, indicating that only one product was generated from **1** upon binding to Co^{2+}. The peak at 400 nm with the high molar extinction coefficient, $8.65 \times 10^3\ M^{-1}\ cm^{-1}$, is too large to be Co-based d–d transitions according to the literatures.[61–63] Therefore, the new peak might be attributed to a ligand-to-metal charge-transfer (LMCT).

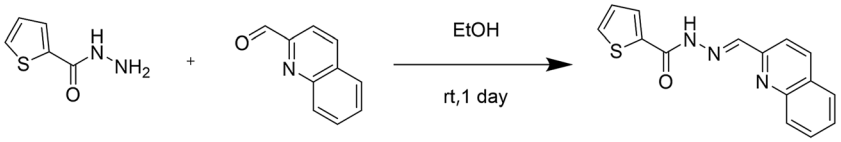

Scheme 1 Synthesis of **1**.

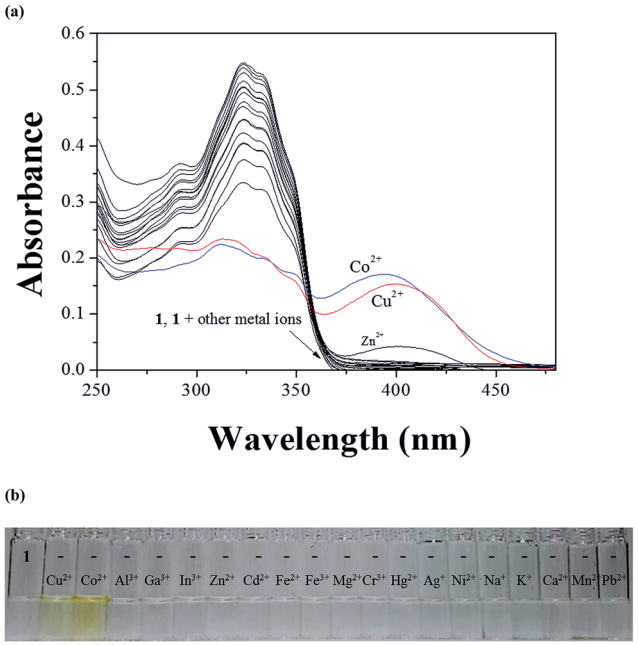

Fig. 1 (a) Absorption spectral changes of **1** (20 μM) upon the addition of various metal ions (0.75 equiv.) in bis–tris buffer/DMSO solution (v/v, 95 : 5). (b) The color changes of **1** (20 μM) upon addition of various metal ions (0.75 equiv.) in bis–tris buffer/DMSO solution (v/v, 95 : 5).

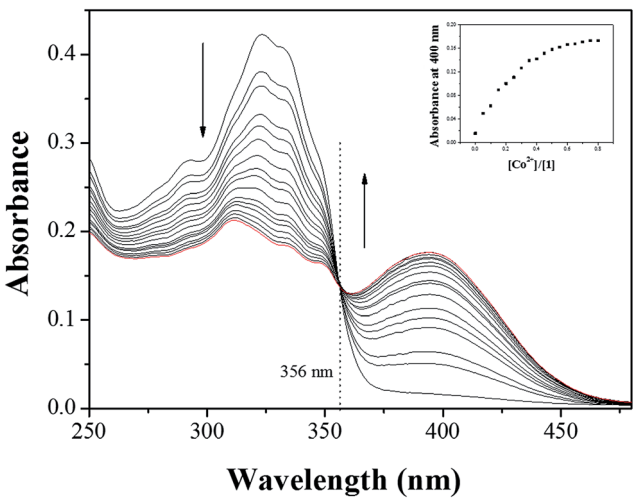

Fig. 2 Absorption spectral changes of **1** (20 μM) after addition of increasing amounts of Co^{2+} in bis–tris buffer/DMSO (95/5, v/v) at room temperature. Inset: absorption at 400 nm *versus* the number of 0.8 equiv. of Co^{2+} added.

The binding mode between **1** and Co^{2+} was determined through job plot analysis (Fig. S1†),[64] which displayed a 2 : 1 stoichiometry. To further confirm the binding mode of Co^{2+}-2·**1** complex, ESI-mass spectrometry analysis was carried out (Fig. 3). The positive-ion mass spectrum showed that the peak at m/z = 620.00 was assignable to $[2\cdot\mathbf{1} + Co^{2+} - H]^+$ [calcd 620.05]. Based on job plot and ESI-mass spectrometry analysis, we proposed the structure of Co^{2+}-2·**1** complex as shown in Scheme 2.

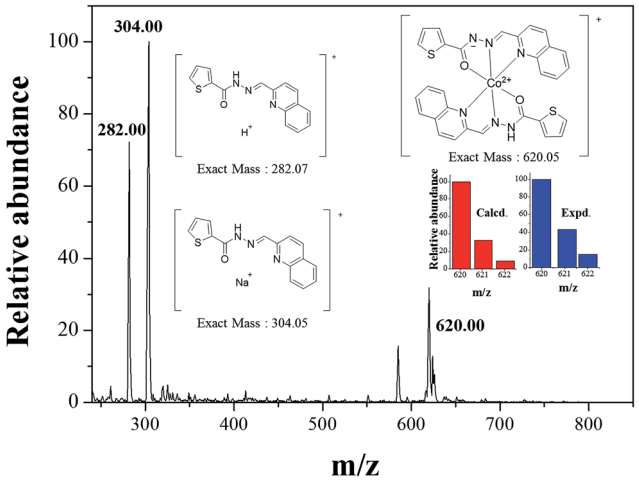

Fig. 3 Positive-ion electrospray ionization mass spectrum of **1** (10 μM) upon addition of 1 equiv. of Co^{2+}.

Based on UV-vis titration data, the association constant of **1** for Co^{2+} was calculated to be 1.0×10^{10} M^{-2} by Li's equations (Fig. S2†),[65] which is within the range of those (10^4–10^{22}) reported for Co^{2+} sensing chemosensors.[61,66,67] The limit of detection was calculated to be 0.19 μM on the basis of 3σ/slope (Fig. S3†),[68] which is lower than the guideline of the New Jersey Ground Water Quality Standards rules (1.7×10^{-6} M).[69] Importantly, the detection limit is the lowest one among those previously reported for simultaneous sensing of Co^{2+} and Cu^{2+} in aqueous solution with more than 90% of water, to the best of our knowledge (Table S1†).[70,71] Thus, the sensor **1** could be a powerful tool for the detection of cobalt in groundwater.

To investigate any interference from various competing metal ions in the detection of Co^{2+}, the competition experiment was executed in the presence of Co^{2+} mixed with various metal ions (Fig. 4). Significantly, no interference was observed for the detection of Co^{2+} from Al^{3+}, Ga^{3+}, In^{3+}, Zn^{2+}, Cd^{2+}, Cu^{2+}, Fe^{2+}, Fe^{3+}, Mg^{2+}, Cr^{3+}, Hg^{2+}, Ag^{+}, Ni^{2+}, Na^{+}, K^{+}, Ca^{2+}, Mn^{2+} and Pb^{2+}. These results indicated that **1** could be an excellent colorimetric sensor for Co^{2+} over competing relevant metal ions in aqueous solution.

For environmental applications, pH effect on the absorption response of sensor **1** to Co^{2+} ion was studied in a series of solutions with pH values ranging from 2 to 12 (Fig. S4†). The color of the Co^{2+}-2·**1** complex remained in the yellow region between pH 7.0 and 11.0. These results indicated that the sensor **1** could clearly detect Co^{2+} by the naked eye or UV-vis absorption measurements over a wide pH range of 7.0–11.0. Moreover, the reusability of sensor **1** was examined by adding ethylenediaminetetraacetic acid (EDTA) to the complexed solution of **1** and Co^{2+}. The spectral changes were reversible after the alternating successive addition of Co^{2+} and EDTA (Fig. S5†). Therefore, sensor **1** toward Co^{2+} could be recyclable by using a suitable reagent such as EDTA.

For quantitative measurement of Co^{2+} in real samples, we constructed a calibration curve for the determination of Co^{2+} (Fig. S6†). Sensor **1** exhibited a good linear relationship between

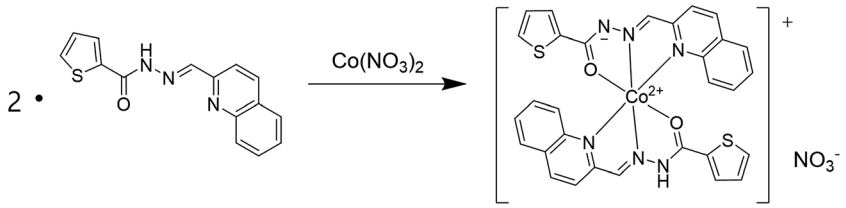

Scheme 2 Proposed binding mode of Co^{2+}-2·**1** complex.

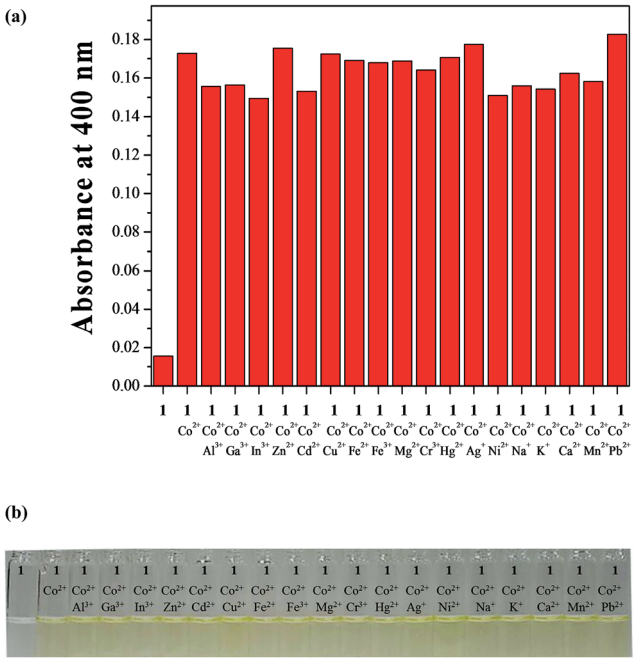

Fig. 4 (a) Absorption spectral changes of competitive selectivity of **1** (20 μM) toward Co^{2+} (0.75 equiv.) in the presence of other metal ions (0.75 equiv.) in bis–tris buffer/DMSO (95/5, v/v). (b) The color changes of competitive selectivity of **1** (20 μM) toward Co^{2+} (0.75 equiv.) in the presence of other metal ions (0.75 equiv.).

the absorbance of **1** and Co^{2+} concentration (0–3 μM) with a correlation coefficient of $R^2 = 0.9902$ ($n = 3$). Based on the calibration curve, the chemosensor was applied for the determination of Co^{2+} in drinking and tap water samples. As shown in Table 1, the satisfactory recoveries and R.S.D. values were obtained for the water samples.

Next, we carried out the UV-vis titration to examine the concentration-dependent signaling of **1** toward Cu^{2+} ion (Fig. 5).

Table 1 Determination of Co^{2+} in water samples[a]

Sample	Co(II) added (μmol L^{-1})	Co(II) found (μmol L^{-1})	Recovery (%)	R.S.D ($n = 3$) (%)
Drinking water	0.00	0.00	—	—
	2.00	2.08	104.0	0.66
Tap water	0.00	0.00	—	—
	2.00	1.89	94.5	1.43

[a] Condition: [**1**] = 20 μmol L^{-1} in bis–tris buffer/DMSO (95/5, v/v).

Upon the gradual addition of Cu^{2+} to a solution of **1**, the absorption band at 325 nm significantly decreased, and a new band at 400 nm gradually increased up to 0.7 equiv. of Cu^{2+}. A clear isosbestic point was also observed 357 nm, which means that only one product was generated from **1** upon binding to Cu^{2+}.

The binding mode between **1** and Cu^{2+} was determined through job plot analysis (Fig. S7†).[64] It displayed a 2 : 1 complexation stoichiometry between **1** and Cu^{2+}. To further understand the binding mode of **1** with Cu^{2+}, ESI-mass spectrometry analysis was carried out (Fig. 6). The positive-ion mass spectrum showed that the peak at $m/z = 624.00$ was assignable to $[(2\cdot\mathbf{1} + Cu^{2+} - H)]^+$ [calcd 624.05].

Through the UV-vis titration data, the association constant of **1** and Cu^{2+} was determined as 7.0×10^9 M^{-1} on the basis of Li's equations (Fig. S8†).[65] The value is within those (10^3–10^{12}) reported for Cu^{2+} sensing chemosensors.[72–77] The detection limit of Cu^{2+} by **1**, on the basis of 3σ/slope,[68] was determined to be 0.13 μM (Fig. S9†). Importantly, the value is much lower than the World Health Organization (WHO) guideline (31.5 μM) for Cu^{2+} in the drinking water.[33,78] Importantly, the detection limit is also the lowest one among those previously reported for simultaneous detection of Co^{2+} and Cu^{2+} by organo-chemosensors in aqueous solution with more than 90% of water, to the best of our knowledge (Table S1†), while a few of

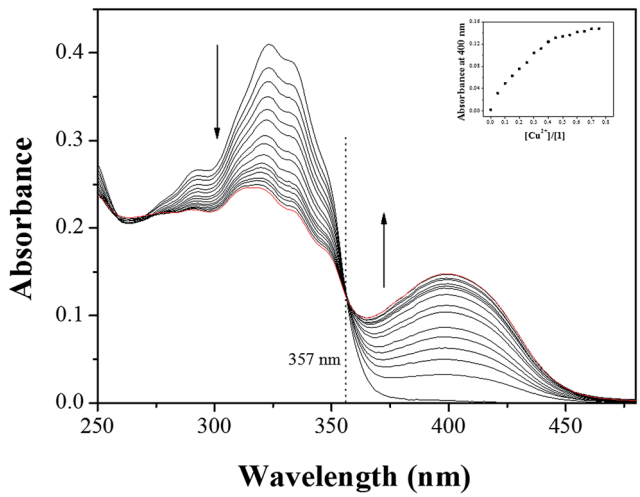

Fig. 5 Absorption spectral changes of **1** (20 μM) after addition of increasing amounts of Cu^{2+} in bis–tris buffer/DMSO (95/5, v/v) at room temperature. Inset: absorption at 400 nm *versus* the number of 0.75 equiv. of Cu^{2+} added.

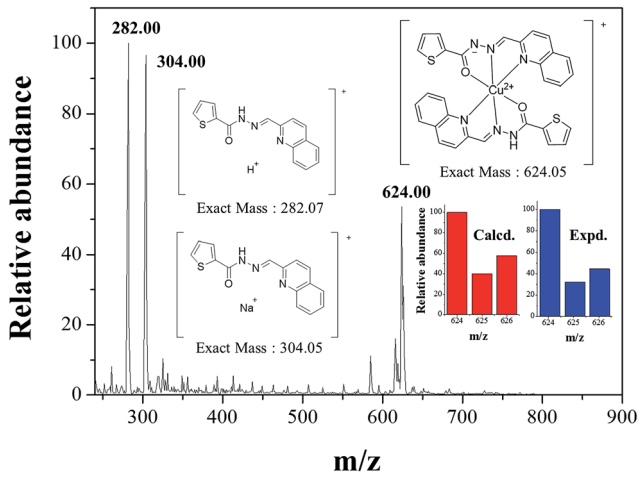

Fig. 6 Positive-ion electrospray ionization mass spectrum of **1** (10 μM) upon addition of **1** equiv. of Cu^{2+}.

inorganic- and nano-materials show better detection limits.[70,71,79,80]

To check the practical applicability of sensor **1** as a Cu^{2+} selective sensor, the competition experiment was conducted by the addition of Cu^{2+} ions (0.7 equiv.) to the solution of **1** containing various metal ions (0.7 equiv.) (Fig. S10†). There was no or slight interference in the detection of Cu^{2+} from the metal ions. For example, Mg^{2+}, Cr^{3+}, Hg^{2+}, Na^{+}, and K^{+} showed the slight interference, but the color of Cu^{2+}-2·**1** complex was still discernible. Thus, **1** could be used as a selective colorimetric sensor for Cu^{2+} in the presence of most competing metal ions.

In order to apply to environmental systems, the effect of pH on the absorption response of sensor **1** to Cu^{2+} was examined at pH values ranging from 2 to 12. As shown in Fig. S11,† sensing ability of **1** for Cu^{2+} was maintained between pH 7.0 and 10.0. This result assured of its application under physiological conditions, without any change in the detection of Cu^{2+}.

For the reversibility test of sensor **1** toward Cu^{2+}, ethylenediaminetraacetic acid (EDTA, 0.7 equiv.) was added to the complexed solution of sensor **1** and Cu^{2+} (Fig. S12†). The absorbance changes were almost reversible after several cycles with the sequentially alternative addition of Cu^{2+} and EDTA. These results showed that sensor **1** toward Cu^{2+} could be recyclable simply through treatment with a proper reagent such as EDTA. Therefore, reversibility and regeneration of sensor **1** could be applicable to the fabrication of chemosensor to detect Cu^{2+}.

Table 2 Determination of Cu^{2+} in water samples[a]

Sample	Cu(II) added (μmol L^{-1})	Cu(II) found (μmol L^{-1})	Recovery (%)	R.S.D (n = 3) (%)
Drinking water	0.00	0	—	—
	2.00	2.10	105.0	4.06
Tap water	0.00	0.00	—	—
	2.00	2.11	105.5	2.74

[a] Condition: [**1**] = 20 μmol L^{-1} in bis–tris buffer/DMSO (95/5, v/v).

In order to examine the practical properties of the chemosensor **1** in environmental samples, the chemosensor **1** was applied for the determination of Cu^{2+} in water samples, using the calibration curve of **1** toward Cu^{2+} (Fig. S13†). Drinking and tap water samples were chosen. As shown in Table 2, appropriate recoveries and R.S.D values of the water samples were obtained.

3.2. Theoretical calculations for 1 and Cu^{2+}-2·1 complex

For a better understanding of the colorimetric sensing mechanism of **1** for Cu, theoretical calculations for **1** and Cu^{2+}-2·**1** were carried out in parallel to the experimental studies. Based on job plot and ESI-mass analysis, all calculations were conducted with a 2 : 1 binding mode of **1** to Cu^{2+}. Under these

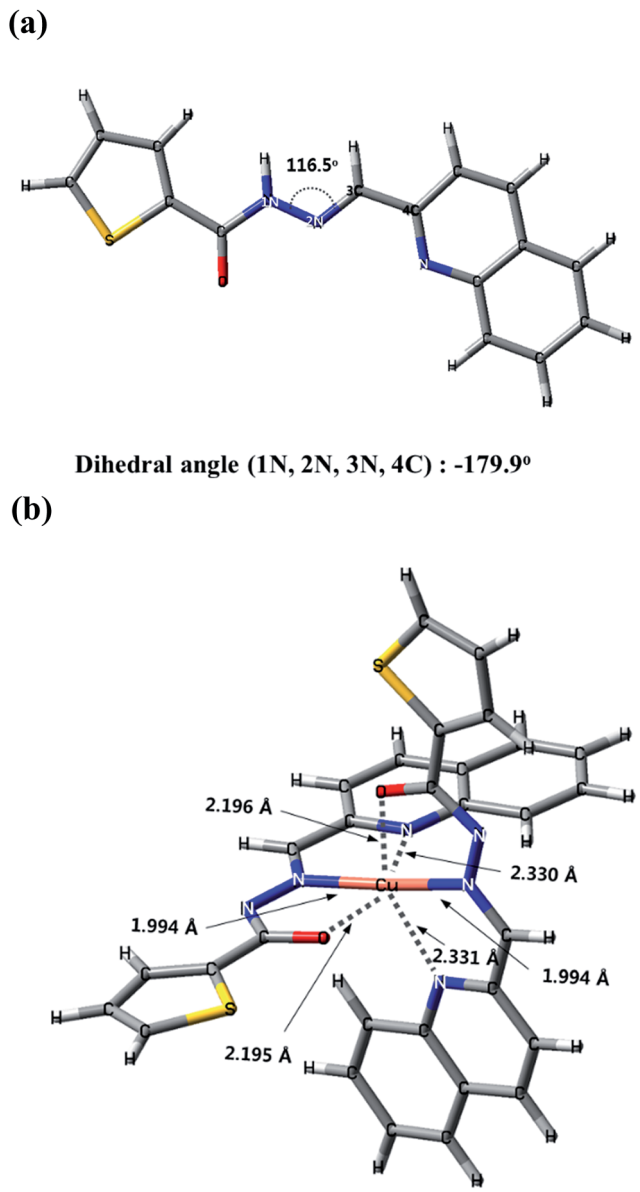

Fig. 7 The energy-minimized structures of (a) **1** and (b) Cu^{2+}-2·**1** complex.

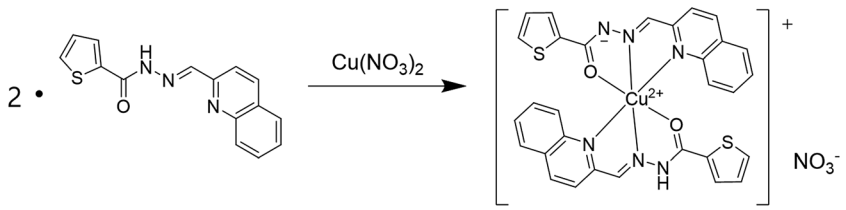

Scheme 3 Proposed binding mode of Cu^{2+}-2·**1** complex.

conditions, geometric optimizations and theoretical calculations of **1** and Cu^{2+}-2·**1** complex were carried out by applying density functional theory (DFT/B3LYP/main group atom: 6-31G** and Cu:Lanl2DZ/ECP). The energy-minimized structures with the significant structural properties are presented in Fig. 7. Sensor **1** was coordinated to Cu^{2+} *via* the O atom in the hydroxyl group and the N atoms in the imine and quinolone. The absorptions to the singlet excited states of **1** and Cu^{2+}-2·**1** complex were investigated using the TD/DFT calculations. Theoretical calculation data of **1** and Cu^{2+}-2·**1** were well matched with those obtained from their UV-vis absorption spectra. For **1**, the main molecular orbital (MO) contribution of the first lowest excited state was determined for HOMO → LUMO transition (346.8 nm), which could be characterized by intramolecular charge transfer (ICT) (Fig. S14†). For Cu^{2+}-2·**1** complex, the MO contributions of the 14th and 16th lowest excited state were described in Fig. S15,† which could be characterized by ICT and ligand-to-metal charge-transfer (LMCT) transitions. Hence, these results indicated that the chelation of **1** to Cu^{2+} might induce the ICT and slight LMCT, which caused the red-shift (346.8 nm → 432.6 and 435.8 nm) with color change from colorless to yellow. Based on job plot, ESI-mass spectrometry analysis, theoretical calculations and the structures reported to literatures,[47,63] we proposed the structure of Cu^{2+}-2·**1** complex as shown in Scheme 3.

3.3. Absorption spectroscopic studies of Co^{2+}-2·1 complex toward CN^-

Some metal complexes showed the selectivity toward specific anions in the systems such as Cu–S, Cu–CN, and Hg–I.[40,81,82] Therefore, we also examined the selectivity of Co^{2+}-2·**1** and Cu^{2+}-2·**1** complexes toward various anions. When 30 equiv. of various anions such as CN^-, OAc^-, F^-, Cl^-, Br^-, I^-, $H_2PO_4^-$, BzO^-, N_3^-, SCN^-, NO_3^- and S^{2-} were added to the two complexes in bis–tris buffer/DMSO (95/5, v/v, pH = 7), only CN^- showed an instant selectivity to Co^{2+}-2·**1** complex (Fig. 8). Both UV-vis spectral and color changes from yellow to colorless were observed for CN^-. These results indicated that Co^{2+}-2·**1** complex can serve as a "naked-eye" chemosensor for CN^- in aqueous solution.

In order to understand the binding properties of Co^{2+}-2·**1** complex with CN^-, we carried out the UV-vis titration

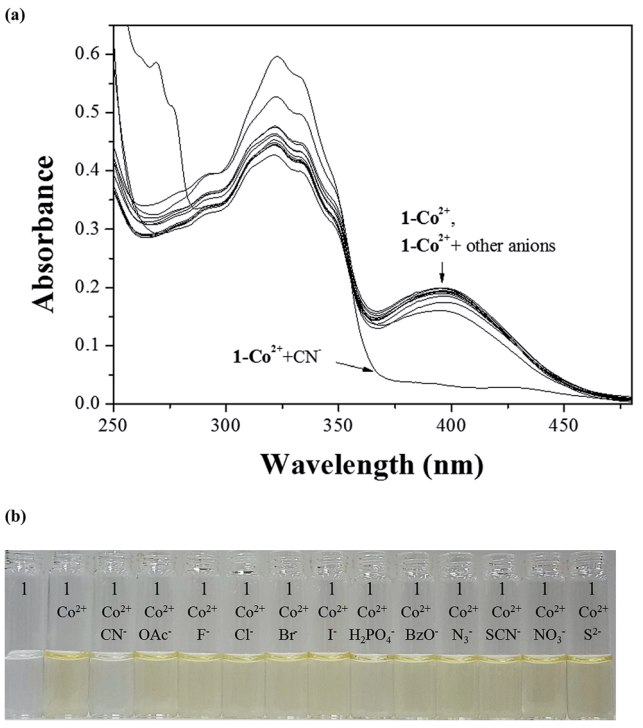

Fig. 8 (a) Absorption spectral changes of the Co^{2+}-2·**1** complex (20 μM) in the presence of 30 equiv. of different anions in bis–tris buffer/DMSO (95/5, v/v). (b) The color changes of the Co^{2+}-2·**1** complex (20 μM) upon addition of various anions (30 equiv.) in bis–tris buffer/DMSO (95/5, v/v).

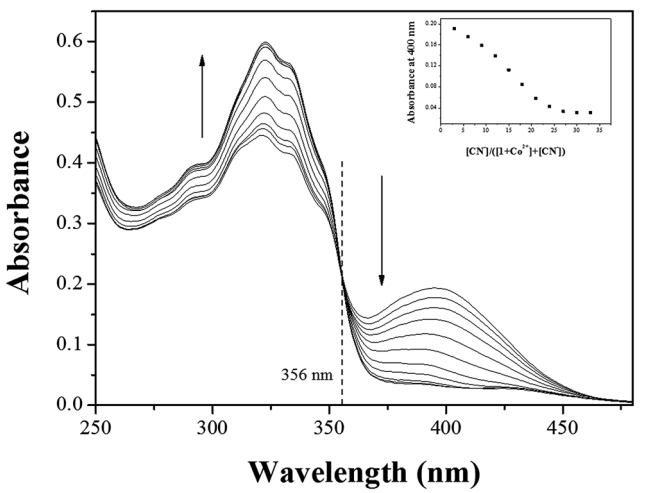

Fig. 9 Absorption spectral changes of Co^{2+}-2·**1** complex (20 μM) upon addition of CN^- (up to 33 equiv.) in bis–tris buffer/DMSO (95/5, v/v). Inset: absorption at 400 nm *versus* the number of equiv. of Co^{2+} added.

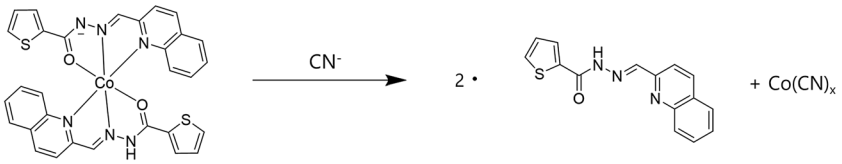

Scheme 4 Proposed sensing mechanism of CN^- by Co^{2+}-2·**1** complex.

experiments (Fig. 9). On the treatment with CN^- to the solution of Co^{2+}-2·**1**, the absorption band at 400 nm significantly decreased, and the band at 325 nm increased with a distinct isosbestic point at 356 nm, indicating the formation of only one UV-active species. Moreover, the final UV-vis spectrum of Co^{2+}-2·**1** with CN^- was nearly identical to that of **1** (Fig. S16†), indicating the reproduction of **1**. These results led us to propose that Co^{2+}-2·**1** complex might undergo the demetallation by CN^- as shown in Scheme 4.

The job plot for the binding between Co^{2+}-2·**1** complex and CN^- revealed a 1 : 1 stoichiometry (Fig. S17†). The binding constant between Co^{2+}-2·**1** and CN^- was calculated as 3.0×10^4 M^{-1} on the basis of the Benesi–Hildebrand equation (Fig. S18†).[83] Based on the result of UV-vis titration, the detection limit for CN^- was determined to be 24.11 μM on basis of 3 σ/K (Fig. S19†).[68] Importantly, this is the third example of the cyanide-selective colorimetric chemosensor by using cobalt complex as a sensor in aqueous solution with more than 90% of water, to best of our knowledge (Table S2†).

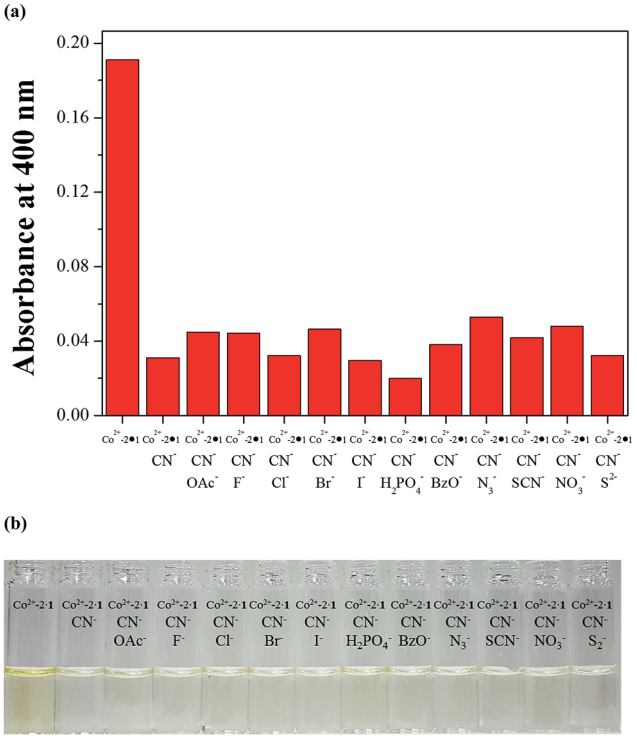

Fig. 10 (a) Absorption spectral changes of competitive selectivity of Co^{2+}-2·**1** complex (20 μM) toward CN^- (30 equiv.) in the presence of other anions (30 equiv.) in bis–tris buffer/DMSO (95/5, v/v). (b) The color changes of competitive selectivity of Co^{2+}-2·**1** complex (20 μM) toward CN^- (30 equiv.) in the presence of other anions (30 equiv.).

To check further the practical applicability of Co^{2+}-2·**1** as a CN^--selective sensor, competition experiments were carried out. For the competition test, the Co^{2+}-2·**1** complex was treated with 30 equiv. of CN^- in the presence of various competing anions (30 equiv.) such as OAc^-, F^-, Cl^-, Br^-, I^-, $H_2PO_4^-$, BzO^-, N_3^-, SCN^-, NO_3^- and S^{2-} in bis–tris buffer/DMSO (95/5, v/v, pH = 7) (Fig. 10). The coexistent anions showed no interference in the UV-vis spectral and color changes for the detection of CN^-. These results suggested that Co^{2+}-2·**1** could be an excellent chemosensor for the detection of CN^- over competing anions through naked eye.

In order to investigate pH dependence of Co^{2+}-2·**1** toward CN^-, the pH test was carried out in a wide range of pH (Fig. S20†). The optimal range for the colorimetric sensing of CN^- by Co^{2+}-2·**1** was turned out to be between pH 7.0 and pH 11.0. Therefore, CN^- could be clearly detected by the naked eye or UV-vis absorption measurements using Co^{2+}-2·**1** over a range of pH 7.0–11.0.

4. Conclusion

We developed a simple thiophene-2-carbohydrazide-based colorimetric chemosensor **1** for Co^{2+} and Cu^{2+}. The sensor **1** selectively detected Co^{2+} and Cu^{2+} through a color change from colorless to yellow. Importantly, **1** could quantify Co^{2+} and Cu^{2+} in real water samples with the satisfactory recoveries and R.S.D values. The binding of **1** with Co^{2+} and Cu^{2+} was reversible with a suitable reagent such as EDTA. In addition, the resulting Co^{2+}-2·**1** complex can be used as a colorimetric sensor for cyanide with changing its color form yellow to colorless in aqueous solution. The cyanide-sensing mechanism by Co^{2+}-2·**1** complex was proposed to be a simple demetallation between Co^{2+}-2·**1** and CN^-. Therefore, these results may contribute to the development of a novel type of chemosensors for a multifunctional "naked-eye" detection of Co^{2+} and Cu^{2+} and for the sequential recognition of Co^{2+} and CN^- by a colorimetric method in aqueous solution.

Acknowledgements

Financial support from Basic Science Research Program through the National Research Foundation of Korea (NRF) funded by the Ministry of Education, Science and Technology (NRF-2014R1A2A1A11051794 and NRF-2015R1A2A2A09001301) are gratefully acknowledged. This subject is also supported by Korea Ministry of Environment (MOE) as "The Chemical Accident Prevention Technology Development Project".

References

1 H. N. Kim, M. H. Lee, H. J. Kim, J. S. Kim and J. Yoon, *Chem. Soc. Rev.*, 2008, **37**, 1465–1472.
2 Y. Ding, Y. Tang, W. Zhu and Y. Xie, *Chem. Soc. Rev.*, 2015, **44**, 1101–1112.
3 Y. Xie, P. Wei, X. Li, T. Hong, K. Zhang and H. Furuta, *J. Am. Chem. Soc.*, 2013, **135**, 19119–19122.
4 B. Chen, Y. Ding, X. Li, W. Zhu, J. P. Hill, K. Ariga and Y. Xie, *Chem. Commun.*, 2013, **49**, 10136–10138.
5 Y. Ding, X. Li, T. Li, W. Zhu and Y. Xie, *J. Org. Chem.*, 2013, **78**, 5328–5338.
6 S. Goswami, D. Sen and N. K. Das, *Org. Lett.*, 2010, **12**, 856–859.
7 K. W. Walker and R. A. Bradshaw, *Protein Sci.*, 1998, **7**, 2684–2687.
8 C. Little, S. E. Aakre, M. G. Rumsby and K. Gwarsha, *Biochem. J.*, 1982, **207**, 117–121.
9 M. Dennis and P. E. Kolattukudy, *Proc. Natl. Acad. Sci. U. S. A.*, 1992, **89**, 5306–5310.
10 D. G. Barceloux, *J. Toxicol., Clin. Toxicol.*, 1999, **37**, 201–206.
11 D. Maity, V. Kumar and T. Govindaraju, *Org. Lett.*, 2012, **14**, 6008–6011.
12 C. Y. Li, X. B. Zhang, Z. Jin, R. Han, G. L. Shen and R. Q. Yu, *Anal. Chim. Acta*, 2006, **580**, 143–148.
13 D. Maity, A. Raj, D. Karthigeyan, T. K. Kundu and T. Govindaraju, *RSC Adv.*, 2013, **3**, 16788–16794.
14 S. Y. Lee, J. J. Lee, K. H. Bok, S. Y. Kim and C. Kim, *RSC Adv.*, 2016, **6**, 28081–28088.
15 J. Shi, C. Lu, D. Yan and L. Ma, *Biosens. Bioelectron.*, 2013, **45**, 58–64.
16 Y. Yao, D. Tian and H. Li, *ACS Appl. Mater. Interfaces*, 2010, **2**, 684–690.
17 Y. Tan, J. Yu, Y. Cui, Y. Yang, Z. Wang, X. Hao and G. Qian, *Analyst*, 2011, **136**, 5283–5286.
18 M. Iniya, D. Jeyanthi, K. Krishnaveni and D. Chellappa, *RSC Adv.*, 2014, **4**, 25393–25397.
19 H. Y. Luo, X. B. Zhang, C. L. He, G. L. Shen and R. Q. Yu, *Spectrochim. Acta, Part A*, 2008, **70**, 337–342.
20 A. Léonard and R. Lauwerys, *Mutat. Res., Genet. Toxicol.*, 1990, **239**, 17–27.
21 K. Y. Ryu, S. Y. Lee, D. Y. Park, S. Y. Kim and C. Kim, *Sens. Actuators, B*, 2017, **242**, 792–800.
22 E. J. Song, G. J. Park, J. J. Lee, S. Lee, I. Noh, Y. Kim, S. J. Kim, C. Kim and R. G. Harrison, *Sens. Actuators, B*, 2015, **213**, 268–275.
23 R. Uauy, M. Olivares and M. Gonzalez, *Am. J. Clin. Nutr.*, 1998, **67**, 952–959.
24 D. G. Barceloux, *J. Toxicol., Clin. Toxicol.*, 1999, **37**, 217–230.
25 S. Bothra, R. Kumar, A. Kuwar, N. Singh and S. K. Sahoo, *Mater. Lett.*, 2015, **145**, 34–36.
26 Y. B. Wagh, A. Kuwar, S. K. Sahoo, J. Gallucci and D. S. Dalal, *RSC Adv.*, 2015, **5**, 45528–45534.
27 X. Chen, M. J. Jou, H. Lee, S. Kou, J. Lim, S. W. Nam, S. Park, K. M. Kim and J. Yoon, *Sens. Actuators, B*, 2009, **137**, 597–602.
28 Y. S. Kim, G. J. Park, S. A. Lee and C. Kim, *RSC Adv.*, 2015, **5**, 31179–31188.
29 Y. K. Jang, U. C. Nam, H. L. Kwon, I. H. Hwang and C. Kim, *Dyes Pigm.*, 2013, **99**, 6–13.
30 A. K. Mahapatra, G. Hazra, N. K. Das and S. Goswami, *Sens. Actuators, B*, 2011, **156**, 456–462.
31 S. Goswami, D. Sen, N. K. Das and G. Hazra, *Tetrahedron Lett.*, 2010, **51**, 5563–5566.
32 B. Sarkar, *Chem. Rev.*, 1999, **99**, 2535–2544.
33 K. J. Barnham, C. L. Masters and A. I. Bush, *Nat. Rev. Drug Discovery*, 2004, **3**, 205–214.
34 K. B. Kim, H. Kim, E. J. Song, S. Kim, I. Noh and C. Kim, *Dalton Trans.*, 2013, **42**, 16569–16577.
35 N. Kumari, N. Dey, S. Jha and S. Bhattacharya, *ACS Appl. Mater. Interfaces*, 2013, **5**, 2438–2445.
36 Y. H. Tang, Y. Qu, Z. Song, X. P. He, J. Xie, J. Hua and G. R. Chen, *Org. Biomol. Chem.*, 2012, **10**, 555–560.
37 D. T. Shi, B. Zhang, Y. X. Yang, C. C. Guan, X. P. He, Y. C. Li, G. R. Chen and K. Chen, *Analyst*, 2013, **138**, 2808–28011.
38 L. Tang, P. Zhou, K. Zhong and S. Hou, *Sens. Actuators, B*, 2013, **182**, 439–445.
39 L. Tang and M. Cai, *Sens. Actuators, B*, 2012, **173**, 862–867.
40 L. Tang, M. Cai, Z. Huang, K. Zhong, S. Hou, Y. Bian and R. Nandhakumar, *Sens. Actuators, B*, 2013, **185**, 188–194.
41 X. Lou, J. Qin and Z. Li, *Analyst*, 2009, **134**, 2071–2075.
42 N. Khairnar, K. Tayade, S. K. Sahoo, B. Bondhopadhyay, A. Basu, J. Singh, N. Singh, V. Gite and A. Kuwar, *Dalton Trans.*, 2015, **44**, 2097–2102.
43 J. H. Kang, S. Y. Lee, H. M. Ahn and C. Kim, *Sens. Actuators, B*, 2017, **242**, 25–34.
44 H. J. Lee, S. J. Park, H. J. Sin, Y. J. Na and C. Kim, *New J. Chem.*, 2015, **39**, 3900–3907.
45 Y. K. Tsui, S. Devaraj and Y. P. Yen, *Sens. Actuators, B*, 2012, **161**, 510–519.
46 T. G. Jo, Y. J. Na, J. J. Lee, M. M. Lee, S. Y. Lee and C. Kim, *Sens. Actuators, B*, 2015, **211**, 498–506.
47 G. R. You, G. J. Park, J. J. Lee and C. Kim, *Dalton Trans.*, 2015, **44**, 9120–9129.
48 J. J. Lee, S. Y. Lee, K. H. Bok and C. Kim, *J. Fluoresc.*, 2015, **25**, 1449–1459.
49 M. R. B. Binet, R. Ma, C. W. McLeod and R. K. Poole, *Anal. Biochem.*, 2003, **318**, 30–38.
50 Y. W. Choi, G. J. Park, Y. J. Na, H. Y. Jo, S. A. Lee, G. R. You and C. Kim, *Sens. Actuators, B*, 2014, **194**, 343–352.
51 R. M. Yucel, Y. He and A. M. Zaslavsky, *Stat. Med.*, 2011, **30**, 3447–3460.
52 A. D. Becke, *J. Chem. Phys.*, 1993, **98**, 5648–5652.
53 C. Lee, W. Yang and R. G. Parr, *Phys. Rev. B: Condens. Matter Mater. Phys.*, 1988, **37**, 785–789.
54 P. C. Hariharan and J. A. Pople, *Theor. Chim. Acta*, 1973, **28**, 213–222.
55 M. M. Francl, W. J. Pietro, W. J. Hehre, J. S. Binkley, M. S. Gordon, D. J. DeFrees and J. a. Pople, *J. Chem. Phys.*, 1982, **77**, 3654–3665.
56 W. R. Wadt and P. J. Hay, *J. Chem. Phys.*, 1985, **82**, 284–298.
57 P. J. Hay and W. R. Wadt, *J. Chem. Phys.*, 1985, **82**, 270–283.

58 V. Barone and M. Cossi, *J. Phys. Chem. A*, 1998, **102**, 1995–2001.
59 M. Cossi and V. Barone, *J. Chem. Phys.*, 2001, **115**, 4708–4717.
60 N. M. O'Boyle, A. L. Tenderholt and K. M. Langner, *J. Comput. Chem.*, 2008, **29**, 839–845.
61 J. J. Lee, Y. W. Choi, G. R. You, S. Y. Lee and C. Kim, *Dalton Trans.*, 2015, **44**, 13305–13314.
62 G. J. Park, Y. J. Na, H. Y. Jo, S. A. Lee and C. Kim, *Dalton Trans.*, 2014, **43**, 6618–6622.
63 G. J. Park, J. J. Lee, G. R. You, L. Nguyen, I. Noh and C. Kim, *Sens. Actuators, B*, 2016, **223**, 509–519.
64 P. Job, *Ann. Chim.*, 1928, **9**, 113–203.
65 G. Grynkiewicz, M. Poenie and R. Y. Tsien, *J. Biol. Chem.*, 1985, **260**, 3440–3450.
66 F. A. Abebe, C. S. Eribal, G. Ramakrishna and E. Sinn, *Tetrahedron Lett.*, 2011, **52**, 5554–5558.
67 S. H. Mashraqui, M. Chandiramani, R. Betkar and K. Poonia, *Tetrahedron Lett.*, 2010, **51**, 1306–1308.
68 Y. Shiraishi, S. Sumiya and T. Hirai, *Chem. Commun.*, 2011, **47**, 4953–4955.
69 C. Y. Tsai and Y. W. Lin, *Analyst*, 2013, **138**, 1232–1238.
70 D. Tsoutsi, L. Guerrini, J. M. Hermida-Ramon, V. Giannini, L. M. Liz-Marzán, A. Wei and R. A. Alvarez-Puebla, *Nanoscale*, 2013, **5**, 5841–5846.
71 A. Contino, G. Maccarrone, M. Zimbone, R. Reitano, P. Musumeci, L. Calcagno and I. P. Oliveri, *J. Colloid Interface Sci.*, 2016, **462**, 216–222.
72 Y. H. Lee, N. Park, Y. Bin Park, Y. J. Hwang, C. Kang and J. S. Kim, *Chem. Commun.*, 2014, **50**, 3197–3200.
73 Y. Dai, Y. G. Wang, J. Geng, Y. X. Peng and W. Huang, *Dalton Trans.*, 2014, **43**, 13831–13834.
74 C. B. Huang, H. R. Li, Y. Luo and L. Xu, *Dalton Trans.*, 2014, **43**, 8102–8108.
75 X. Guan, W. Lin and W. Huang, *Org. Biomol. Chem.*, 2014, **12**, 3944–3949.
76 Q. Zou, X. Li and H. Ågren, *Dyes Pigm.*, 2014, **111**, 1–7.
77 S. Pu, L. Ma, G. Liu, H. Ding and B. Chen, *Dyes Pigm.*, 2015, **113**, 70–77.
78 B. Sarkar, *Chem. Rev.*, 1999, **113**, 2535–2544.
79 V. K. Gupta, R. Prasad and A. Kumar, *Talanta*, 2003, **60**, 149–160.
80 A. K. Singh, P. Saxena, S. Mehtab and A. Panwar, *Anal. Bioanal. Chem.*, 2006, **7**, 1342–1346.
81 G. J. Park, I. H. Hwang, E. J. Song, H. Kim and C. Kim, *Tetrahedron*, 2014, **70**, 2822–2828.
82 S. Y. Lee, J. J. Lee, K. H. Bok, J. A. Kim, Y. K. So and C. Kim, *Inorg. Chem. Commun.*, 2016, **70**, 147–152.
83 H. A. Benesi and J. H. Hildebrand, *J. Am. Chem. Soc.*, 1949, **71**, 2703–2707.